Dynamic Characteristics of DC Motor Controlled by Thyristor Chopper Circuit

AUTHOR(S):

ANDO, Tsuguo; MORI, Shinichiro; UMOTO, Juro

CITATION:

ANDO, Tsuguo ...[et al]. Dynamic Characteristics of DC Motor Controlled by Thyristor Chopper Circuit. Memoirs of the Faculty of Engineering, Kyoto University 1982, 44(1): 59-77

ISSUE DATE:

1982-03-25

URL:

http://hdl.handle.net/2433/281200

Dynamic Characteristics of DC Motor Controlled by Thyristor Chopper Circuit

By

Tsuguo ANDO*, Shinichiro MORI* and Juro UMOTO*

(Received September 24, 1981)

Abstract

A theoretical method to analyse the steady and dynamic characteristics of a separately excited dc motor controlled by a thyristor chopper circuit is introduced. In the analysis, the influences of the fluctuations of the dc motor speed and the armature current during one cycle of a chopper frequency on the characteristics are considered. The characteristic equation in the control circuit is derived theoretically, and it is then denoted that the circuit performance can be described by an equivalent sampled data system. Next, the validity of the theoretical method is verified by ascertaining that the calculated results agree well with the experimental results. Furthermore, the influences of the circuit parameters and the situation of an armature current on the motor performances are investigated. Finally, the sampled data system is applied to investigate the frequency response of the motor, which has not been investigated in the usual papers.

1 Introduction

A thyristor chopper circuit is available for obtaining a regulated voltage from a constant dc voltage source. The circuit is often used for the speed control system of a dc motor such as that of an electric motor car. The speed of the dc motor is efficiently controlled by regulating an armature terminal voltage of the motor. When the terminal voltage is regulated by a thyristor chopper circuit, the armature current flows intermittently and so the motor fluctuates a little.

Until now, a considerable amount of information describing the performance of a motor controlled by a chopper circuit has been published. However, the analysis of the characteristics in the steady state has been mostly carried out under an assumption that the fluctuation of the motor speed is negligible. Research reports that have analysed the dynamic characteristics considering the fluctuation are rarely found.

In this paper, a theoretical method to analyse the dynamic and steady performances of a separately excited dc motor controlled by a chopper circuit is

* Department of Electrical Engineering.

introduced. By this theory, the fluctuation of the motor speed, the friction torque of the motor with a load and the voltage drops on the armature brushes are considered. These factors have not been considered by the conventional theory, but they are important for researching the motor performances more exactly. Also introduced theoretically is the idea that the motor performances in the chopper circuit are described by a sampled data system. This sampled data system is available for investigating the dynamic characteristics of the motor such as frequency response.

Furthermore, the authors confirm the appropriateness of their theory by showing that the calculated results agree sufficiently well with the experimental results.

2. Fundamental Theory

2.1 Fundamental equations.

Figure 1 shows a circuit diagram of a thyristor chopper circuit for the speed

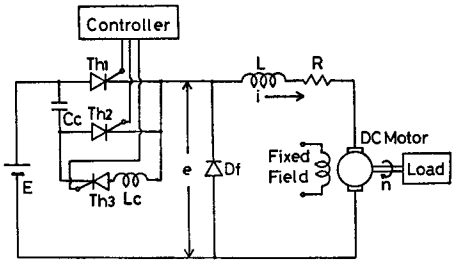

Fig. 1. Chopper control circuit of a separately excited dc motor.

control of a separately excited dc motor, in which the armature terminal voltage e is varied by changing the conduction interval of the main thyristor *Th*1. In the figure, *Th*1 is periodically turned on by gate signals generated in the gate controller, and then the armature current i is supplied to the dc motor from the dc voltage source E. When the auxiliary thyristor *Th*2 is turned on, *Th*1 is soon turned off by the aid of the reverse voltage charged in the condenser Cc, and then the current i transfers from *Th*1 to *Th*2. After a short time i.e. the commutation interval, Cc is recharged with E and so *Th*2 is turned off. Subsequently i circulates through the freewheeling diode *Df* until i decreases to zero, or *Th*1 is turned on again. The polarity of the voltage of Cc is reversed in the resonance circuit consisting of Cc and the inductor Lc when *Th*1 and another auxiliary thyristor *Th*3 are turned on. The reversed voltage of Cc helps to turn *Th*1 off.[1)]

Next, the performance of the dc motor in Fig. 1 can be analysed by the following fundamental equations:

$$\left.\begin{aligned} e &= L\,di/dt+Ri+K_v n+E_b\,, \\ K_t i &= J\,dn/dt+Fn+Q\,, \end{aligned}\right\} \qquad \cdots\cdots(1)$$

where

e : output voltage of chopper circuit,
E_b : brush voltage drop,
F : viscous friction coefficient of motor with load,
J : moment of inertia of the same one,
Q : coulomb torque coefficient of the same one,
K_t : counter electromotive force coefficient of motor,
K_v : torque coefficient of motor,
L : total inductance in armature circuit,
R : total resistance in the same one,
n : motor rotating speed,
t : time.

2.2 Circuit modes.

We now assume that the turn-on and turn-off intervals of the thyristors and the commutation interval of the chopper can be nelgected. Also, for simplifying the analysis of circuit performances, we neglect an armature reaction of the motor and the nonlinearity of the circuit parameters. Then, the Eqs. (1) are transformed into the following electrical equations:

$$\left.\begin{aligned} e &= E_1 H(t)-E_2 H(t') \\ &= L\,di/dt+Ri+v+E_b\,, \\ i &= C\,dv/dt+Gv+I_q\,, \end{aligned}\right\} \qquad \cdots\cdots(2)$$

where

$E_1=E-Eth_1$, $E_2=E-Eth_1+Edf$, $t'=t-t_{on}$,
α : duty factor of chopper,
Eth_1 : voltage drop in $Th1$,
Edf : the same one in Df,
$H(t)$: unit function,
$t_{on}=\alpha\tau$: conduction interval of $Th1$,
τ : chopper period,
$C=J/(K_t K_v)$: equivalent capacitance for J,
$G=F/(K_t K_v)$: equivalent conductance for F,
$I_q=Q/K_t$: equivalent forced current for Q,
$v=K_v n$: counter electromotive force.

Now, we can divide the circuit performances into four fundamental modes, depending on the situation of i and v as follows:[2),3)]

mode 0: $i=0$ and the motor is at a standstill,

mode 1: i is supplied but the driving torque $K_t i$ is not sufficient to rotate the motor,

mode 2: the motor is driven by i,

mode 3: $i=0$ but the motor is rotated by inertia.

The situation of i and v at each mode and the criteria for mode transitions are shown in Fig. 2, where Qs is the static friction torque. The circuit performances in Fig. 1 can be analysed by using Eqs. (2) and Fig. 2. We now show the fundamental relations in each mode.

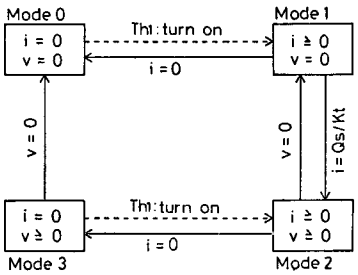

Fig. 2. Circuit modes.

(1) Mode 0

$$e=0\,,\quad i=0\,,\quad v=0\,. \qquad \cdots\cdots(3)$$

(2) Mode 1.

Replacing e, i and v in mode 1 by e_1, i_1 and v_1 respectively, the Eqs. (2) are transformed into

$$\left.\begin{aligned} e_1 &= L\,di_1/dt+Ri_1+E_b\,,\\ v_1 &= 0\,. \end{aligned}\right\} \qquad \cdots\cdots(4)$$

The above equations can be solved easily, and the solutions are expressed by the following matrix form:

$$\begin{bmatrix} i_1 \\ v_1 \end{bmatrix} = [\Phi_1(t)]+[\chi_1(t)]\begin{bmatrix} i_1^{+0} \\ v_1^{+0} \end{bmatrix}, \qquad \cdots\cdots(5)$$

where

$$[\Phi_1(t)] = \begin{bmatrix} \{(E_1-E_b)(1-\varepsilon^{-tR/L})H(t)-E_2(1-\varepsilon^{-t'R/L})H(t')\}/R \\ 0 \end{bmatrix},$$

$$[\chi_1(t)] = \varepsilon^{-tR/L}[U]H(t)\,,$$

$$[U] = \begin{bmatrix} 1 & 0 \\ 0 & 1 \end{bmatrix},$$

i_1^{+0} and $v_1^{+0}=0$: initial values of i_1 and v_1.

(3) Mode 2.

The circuit performance in this mode is described by Eqs. (2). By using the Laplace transform and putting $e=e_2$, $i=i_2$ and $v=v_2$, the Eqs. (2) are easily solved and the solutions are obtained as follows:

$$\begin{bmatrix} i_2 \\ v_2 \end{bmatrix} = [\Phi_2(t)]+[\chi_2(t)]\begin{bmatrix} i_2^{+0} \\ v_2^{+0} \end{bmatrix}, \qquad \cdots\cdots(6)$$

where

$$[\phi_2(t)] = \mathcal{L}^{-1}\left\{\frac{1}{LCD(S)}\begin{bmatrix} SC+G & -1 \\ 1 & SL+R \end{bmatrix}\begin{bmatrix} e_2(S)-E_b(S) \\ -I_q(S) \end{bmatrix}\right\}$$

$$= \begin{bmatrix} (E_1-E_b)\left\{\dfrac{Gg_1(t)}{RG+1}+\dfrac{g_2(t)}{L}\right\}+\dfrac{I_q g_1(t)}{RG+1}-E_2\left\{\dfrac{Gg_1(t')}{RG+1}+\dfrac{g_2(t')}{L}\right\} \\ \dfrac{(E_1-E_b)g_1(t)}{RG+1}-I_q\left\{\dfrac{Rg_1(t)}{RG+1}+\dfrac{g_2(t)}{C}\right\}-\dfrac{E_2 g_1(t')}{RG+1} \end{bmatrix},$$

$$[\chi_2(t)] = \mathcal{L}^{-1}\left\{\frac{1}{D(S)}\begin{bmatrix} S+G/C & -1/L \\ 1/C & S+R/L \end{bmatrix}\right\} = \begin{bmatrix} g_3(t)-\sigma g_2(t) & -g_2(t)/L \\ g_2(t)/C & g_3(t)+\sigma g_2(t) \end{bmatrix},$$

$$g_1(t) = H(t)-\lambda g_2(t)-g_3(t)\,, \qquad \lambda = (R/L+G/C)/2\,,$$

$$g_2(t) = \exp(-\lambda t)\sinh \mu t H(t)/\mu, \qquad \sigma = (R/L-G/C)/2\,,$$

$$g_3(t) = \exp(-\lambda t)\cosh \mu t\, H(t)\,, \qquad \mu = \{\sigma^2-1/(LC)\}^{1/2},$$

$$D(S) = S^2+(R/L+G/C)S+(RG+1)/(LC)\,,$$

$e_2(s)$, $E_b(S)$ and $I_q(S)$: s-functions of e_2, E_b and I_q,

S: Laplace operator,

$\mathcal{L}^{-1}$: inverse Laplace transform,

i_2^{+0} and v_2^{+0}: initial values of i_2 and v_2.

(4) Mode 3.

The circuit equations are given by

$$\left.\begin{aligned} e_3 &= v_3\,, \\ i_3 &= 0 = Cdv_3/dt+Gv_3+I_q\,, \end{aligned}\right\} \qquad \cdots\cdots(7)$$

and the solutions are given by

$$\begin{bmatrix} i_3 \\ v_3 \end{bmatrix} = [\Phi_3(t)]+[\chi_3(t)]\begin{bmatrix} i_3^{+0} \\ v_3^{+0} \end{bmatrix}, \qquad \cdots\cdots(8)$$

where

$$[\phi_3(t)] = \begin{bmatrix} 0 \\ -I_q(1-\varepsilon^{-tG/C})H(t)/G \end{bmatrix},$$

$[\chi_3(t)] = \varepsilon^{-tG/C}[U]H(t)$,

e_3, i_3 and v_3: e, i and v in mode 3,

$i_3^{+0}=0$ and v_3^{+0}: initial values of i_3 and v_3.

3. Steady Characteristics

The steady characteristics of the electro-mechanical system in Fig. 1 can be obtained by analysing the circuit performances during one cycle of the chopper frequency. Here, in the case where the motor rotates continuously, we analyse the circuit performances which are concerned closely with the motor speed control.

We first analyse the circuit performances where i flows interruptedly. During one cycle, modes 2 and 3 appear successively, and so the instantaneous values of i and v are given by Eqs. (6) and (8). In the steady state, the following relations for the initial values are obtained.

$$\begin{bmatrix} i_2^{+0} \\ v_2^{+0} \end{bmatrix} = \begin{bmatrix} i_3 \\ v_3 \end{bmatrix}_{t=t_3}, \quad \begin{bmatrix} i_3^{+0} \\ v_3^{+0} \end{bmatrix} = \begin{bmatrix} i_2 \\ v_2 \end{bmatrix}_{t=t_2} \qquad \cdots\cdots(9)$$

where

$i_2^{+0} = i_3^{+0} = 0$,

$t_2+t_3 = \tau$,

t_r: duration of interval of mode r,

r : mode number.

From Eqs. (6), (8) and (9), we can derive the following equations,

$$\begin{bmatrix} i_2^{+0} \\ v_2^{+0} \end{bmatrix} = \{[U]-[\chi_2(t_3)][\chi_3(t_2)]\}^{-1}\{[\Phi_3(t_3)]+[\chi_3(t_3)][\Phi_2(t_2)]\}, \qquad \cdots\cdots(10)$$

and then the values of t_2, t_3, v_2^{+0} and v_3^{+0} are determined. Therefore, we can calculate the instantaneous values of i and v by substituting those values into Eqs. (6) and (8).

In the case where i flows continuously and only mode 2 appears, the values of i_2^{+0} and v_2^{+0} are obtained by substituting $t_2=\tau$ and $t_3=0$ into Eqs. (10), and then i and v are calculated by using Eqs. (6).

Next, the average values E_d, I_d and V_d per τ of e, i and v can be calculated

easily by using Eqs. (2) and (7). The results bring the following relations:

$$\left.\begin{aligned} E_d &= RI_d+V_d+\beta E_b\,, \\ I_d &= GV_d+I_q\,, \end{aligned}\right\} \qquad \cdots\cdots(11)$$

where

$$E_d = \frac{1}{\tau}\int_0^{\tau} edt = \beta(E_1-E_2)+\alpha E_2-I_q(1-\beta)-(v_2^{+0}-v_3^{+0})C/(G\tau)\,,$$

$$I_d = \frac{1}{\tau}\int_0^{\tau} idt = \frac{1}{\tau}\int_0^{t_2} i_2 dt\,,$$

$$V_d = \frac{1}{\tau}\int_0^{\tau} vdt = \frac{1}{\tau}\left(\int_0^{t_2} v_2 dt+\int_0^{t_3} v_3 dt\right),$$

$$\beta = t_2/\tau\,.$$

Also, about the average input and output powers, the following relations:

$$P_i = P_0+RI_{rms}^2+E_bI_d+\frac{E_{th_1}}{\tau}\int_0^{t_{on}} idt+\frac{E_{df}}{\tau}\int_{t_{on}}^{t_2} idt\,, \qquad \cdots\cdots(12)$$

where

$$P_i = \frac{E}{\tau}\int_0^{t_{on}} idt\text{: average input power,}$$

$$P_0 = \frac{1}{\tau}\int_0^{t_2} vidt\text{: average output power,}$$

$$I_{rms} = \left\{\frac{1}{\tau}\int_0^{t_2} i^2dt\right\}^{1/2}\text{: affective value of } i,$$

are obtained, and those values can be numerically calculated by a digital computer. The electrical efficiency η_e is now determined by

$$\eta_e = P_0/P_i\,. \qquad \cdots\cdots(13)$$

When i flows continuously, η_e is obtained by substituting $t_2=\tau$, $t_3=0$ and $\beta=1$ into Eqs. (12) and (13).

4. Dynamic Characteristics

The dynamic characteristics of the electro-mechanical system in Fig. 1 can be analysed by using Eqs. (3), (4), (6) and (8) and the criteria shown in Fig. 2. For simplifying the analysis, we explain the dynamic characteristics only in the case where the motor rotates continuously and the circuit performance is represented by modes 2 and 3 in every cycle of the chopper frequency.

4.1 Transient characteristics.

In the k-th cycle from a cycle when the duty factor α of the chopper is settled, modes 2 and 3 occur successively in the case where i flows interruptedly. By using Eqs. (6) and (8), the current $i=i_k$ and the voltage $v=v_k$ in the k-th cycle are expressed as follows:

for $0\leq t\leq t_{2,k}\leq\tau$,

$$\begin{bmatrix} i_k \\ v_k \end{bmatrix} = \begin{bmatrix} i_{2,k} \\ v_{2,k} \end{bmatrix} = [\Phi_2(t)]+[\chi_2(t)]\begin{bmatrix} i_{2,k}^{+0} \\ v_{2,k}^{+0} \end{bmatrix}, \qquad \cdots\cdots(14)$$

for $0\leq t\leq t_{3,k}\leq\tau$,

$$\begin{bmatrix} i_k \\ v_k \end{bmatrix} = \begin{bmatrix} i_{3,k} \\ v_{3,k} \end{bmatrix} = [\Phi_3(t)]+[\chi_3(t)]\begin{bmatrix} i_{3,k}^{+0} \\ v_{3,k}^{+0} \end{bmatrix}, \qquad \cdots\cdots(15)$$

where $t_{2,k}$ and $t_{3,k}$ are the duration of modes 2 and 3, respectively. In the above equations, the following conditions

$$\left.\begin{aligned} &\begin{bmatrix} i_{2,k}^{+0} \\ v_{2,k}^{+0} \end{bmatrix} = \begin{bmatrix} i_{3,k-1} \\ v_{3,k-1} \end{bmatrix}_{t=t_{3,k-1}}, \quad \begin{bmatrix} i_{3,k}^{+0} \\ v_{3,k}^{+0} \end{bmatrix} = \begin{bmatrix} i_{2,k} \\ v_{2,k} \end{bmatrix}_{t=t_{2,k}}, \\ &i_{2,k}^{+0} = i_{3,k}^{+0} = 0, \\ &t_{2,k}+t_{3,k} = \tau, \end{aligned}\right\} \qquad \cdots\cdots(16)$$

must be satisfied.

Next, when i flows continuously, $i=i_k$ and $v=v_k$ are expressed by

$$\begin{bmatrix} i_k \\ v_k \end{bmatrix} = \begin{bmatrix} i_{2,k} \\ v_{2,k} \end{bmatrix} = [\Phi_2(t)]+[\chi_2(t)]\begin{bmatrix} i_{2,k}^{+0} \\ v_{2,k}^{+0} \end{bmatrix}, \qquad \cdots\cdots(17)$$

in which

$$\begin{aligned} \begin{bmatrix} i_{2,k}^{+0} \\ v_{2,k}^{+0} \end{bmatrix} &= \begin{bmatrix} i_{2,k-1} \\ v_{2,k-1} \end{bmatrix}_{t_2=\tau} \\ &= \{[U]-[\chi_2(\tau)]\}^{-1}\{[U]-[\chi_2(\tau)]^{k-1}\}[\Phi_2(\tau)]+[\chi_2(\tau)]^{k-1}\begin{bmatrix} i_{2,1}^{+0} \\ v_{2,1}^{+0} \end{bmatrix}. \end{aligned} \qquad \cdots\cdots(18)$$

4.2 Transfer function.

When the dc motor is driven by a dc source, the transfer function $G_d(S)$ of the system is usually expressed as follows:[4]

$$G_d(S) = \frac{\Delta v(S)}{\Delta e(S)} = \frac{1}{RG+1}\,\frac{(RG+1)/(LC)}{D(S)} \qquad \cdots\cdots(19)$$

where

$D(S) = S^2+(R/L+G/C)S+(RG+1)/(LG)$,

Δe : increment of e,

Δv : increment of v caused by Δe,

Here, let us introduce the theoretical transfer function $G(S)$ in the case where the *dc* motor is driven by the chopper circuit, and α is changed $\Delta\alpha$. When i flows continuously and only mode 2 occurs, the characteristic equation $D(S)=0$ is the same as in Eq. (19). However, when i flows interruptedly, $D(S)$ is not decided exactly, because the circuit operations are divided into modes 2 and 3. Hence, we introduce the approximate characteristic equation and then the transfer function.

Let us assume that the circuit situation for α is in the steady state, and so the values of $i^{+0}=i_2^{+0}$, $v^{+0}=v_2^{+0}$, t_2 and t_3 are determined by Eqs. (10). We also assume that the variation $\Delta\alpha$ is very small, and so the durations t_2 and t_3 for $\alpha+\Delta\alpha$ are nearly equal to those for α. Then, we can solve the following gradual equations for $\alpha+\Delta\alpha$.

$$\begin{bmatrix} i_{2,k}^{+0} \\ v_{2,k}^{+0} \end{bmatrix} = \begin{bmatrix} i_{3,k-1} \\ v_{3,k-1} \end{bmatrix}_{t=t_3}, \quad \begin{bmatrix} i_{3,k}^{+0} \\ v_{3,k}^{+0} \end{bmatrix} = \begin{bmatrix} i_{2,k} \\ v_{2,k} \end{bmatrix}_{t=t_2}. \qquad \cdots\cdots(20)$$

By using Eqs. (14) and (15), the following result is derived.

$$\begin{bmatrix} i_{2,k}^{+0} \\ v_{2,k}^{+0} \end{bmatrix} = \{[U]-[\chi_3(t_3)]\,[\chi_2(t_2)]\}^{-1}\{[U]-[\chi_3(t_3)]^{k-1}[\chi_2(t_2)]^{k-1}\}$$
$$\times\{[\Phi_3(t_3)]+[\chi_3(t_3)]\,[\Phi_2(t_2)]_{\alpha=\alpha+\Delta\alpha}\}+[\chi_3(t_3)]^{k-1}[\chi_2(t_2)]^{k-1}\begin{bmatrix} i_{2,1}^{+0} \\ v_{2,1}^{+0} \end{bmatrix} \qquad \cdots\cdots(21)$$

In the above equation, the transient term $[\chi_3(t_3)]^{k-1}[\chi_2(t_2)]^{k-1}$ can be given as follows;

$$[\chi_3(t_3)]^{k-1}[\chi_2(t_2)]^{k-1} = [\chi_3(\overline{k-1}t_3)]\,[\chi_2(\overline{k-1}t_2)]$$
$$= \frac{\varepsilon^{-(k-1)t_3G/C}}{S_1-S_2}\left\{\varepsilon^{(k-1)t_2S_1}\begin{bmatrix} S_1+G/C & -1/L \\ 1/C & S_1+R/L \end{bmatrix}\right.$$
$$\left.-\varepsilon^{(k-1)t_2S_2}\begin{bmatrix} S_2+G/C & -1/L \\ 1/C & S_2+R/L \end{bmatrix}\right\}, \qquad \cdots\cdots(22)$$

where $S_1=-\lambda+\mu$ and $S_2=-\lambda-\mu$ are the solutions of $D(S)=0$. By using the parameters $\beta=t_2/\tau$, $S_1'=\beta S_1-(1-\beta)G/C$, $S_2'=\beta S_2-(1-\beta)G/C$, $L'=L/\beta$, $C'=C/\beta$ and $R'=R+(1-\beta)\,LG/(\beta C)$, the Eqs. (22) are transformed into

$$[\chi_3(t_3)]^{k-1}[\chi_2(t_2)]^{k-1} = \frac{1}{S_1'-S_2'}\left\{\varepsilon^{(k-1)\tau S_1'}\begin{bmatrix} S_1'+G'/C' & -1/L' \\ 1/C & S_1'+R'/L' \end{bmatrix}\right.$$
$$\left.-\varepsilon^{(k-1)\tau S_2}\begin{bmatrix} S_2'+G'/C' & -1/L' \\ 1/C' & S_2'+R'/L' \end{bmatrix}\right\}. \qquad \cdots\cdots(23)$$

Furthermore, the above transient term can be expressed by the following inverse Laplace transformation

$$[\chi_3(t_3)]^{k-1}[\chi_2(t_2)]^{k-1} = \mathcal{L}^{-1}\left\{\frac{1}{D'(S)}\begin{bmatrix} S+G'/C' & -1/L' \\ 1/C' & S+R'/L' \end{bmatrix}\right\}_{t=(k-1)\tau} \quad \cdots\cdots(24)$$

where

$$D'(S) = S^2+(R'/L'+G'/C')S+(R'G'+1)/(L'C') \quad \cdots\cdots(25)$$

In the equation, $D'(S)$ is the same form as $D(S)$ in Eq. (19), and $D'(S)=0$ is now an approximate characteristic equation in the case where i flows interruptedly. In this connection, by putting $t_3=0$ and $t_2=\tau$, i.e. $\beta=1$, in Eqs. (23), we can obtain the transient term $[\chi_2(\tau)]^{k-1}$ in Eqs. (18), and then $D'(S)=D(S)$.

Next, the gain K_m of the motor for $\Delta\alpha$ can be obtained by using Eqs. (10), and is expressed as

$$K_m = \frac{\Delta v^{+0}}{\Delta\alpha} = \frac{\partial v_2^{+0}}{\partial\alpha}+\frac{\partial v_2^{+0}}{\partial t_2}\frac{\partial t_2}{\partial\alpha}+\frac{\partial v_2^{+0}}{\partial t_3}\frac{\partial t_3}{\partial\alpha} \quad \cdots\cdots(26)$$

where

$\Delta v^{+0}=\Delta v_2^{+0}$: change of the initial value of v due to $\Delta\alpha$.

Now, K_m and $D'(S)$ are determined, and the transfer function $G(S)$ of the motor control circuit with the chopper is written by

$$G(S) = \frac{\Delta v^{+0}(S)}{\Delta\alpha(S)} = K_m\frac{(R'G'+1)/(L'C')}{D'(S),} \quad \cdots\cdots(27)$$

This is transformed into the following expression:

$$G(S) = \frac{K_m\omega_n^2}{S^2+\zeta\omega_n S+\omega_n^2}, \quad \cdots\cdots(28)$$

where

$\omega_n = \{(R'G'+1)/(L'C')\}^{1/2}$: natural angular frequency,
$\zeta = (R'/L'+G'/C')/(2\omega_n)$: attenuation constant.

The transfer function $G(S)$ is very useful to analyse dynamic characteristics of the motor.

4.3 Pulse transfer function.

When the motor speed is controlled by the feedback control system, the dynamic characteristic is derived from the equivalent sampled data system, as shown in Fig. 3. In the figure, the zero order holding circuit

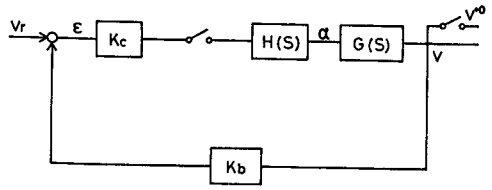

Fig. 3. Equivalent sampled data system with speed feedback.

$$H(S) = \frac{1-\varepsilon^{-\tau s}}{S}, \qquad \cdots\cdots(29)$$

is used, because α is periodically given to the chopper circuit and is kept constant during τ. Also, K_c and K_b are the gains in the controller and the feedback circuit, respectively, v_r is the input signal for speed control, and $\varepsilon = v_r - v$.

In order to analyse the dynamic characteristic of the system as shown in Fig. 3, it is convenient to use a pulse transfer function. The total pulse transfer function $G_t^*(z)$ of the system is given by[5]

$$\begin{aligned} G_t^*(z) &= \frac{K_c HG^*(z)}{1+K_b K_c HG^*(z)} \\ &= \frac{N_1 z+N_2}{M_1 z^2+M_2 z+M_3}, \end{aligned} \qquad \cdots\cdots(30)$$

where

$$\begin{aligned} M_1 &= S_1' S_2' (S_1'-S_2'), \\ M_2 &= -M_1(\varepsilon^{\tau S_1'}+\varepsilon^{\tau S_2'})+K_b N_1, \\ M_3 &= M_1 \varepsilon^{\tau(S_1'+S_2')}+K_b N_2, \\ N_1 &= K_c K_m (S_1'-S_2'-S_1'\varepsilon^{\tau S_2'}+S_2'\varepsilon^{\tau S_1'}), \\ N_2 &= K_c K_m \{S_2'\varepsilon^{\tau S_2'}-S_1'\varepsilon^{\tau S_1'}+(S_1'-S_2')\varepsilon^{\tau(S_1'+S_2')}\}, \\ S_1' &= -\zeta\omega_n+\omega_n(\zeta^2-1)^{1/2}, \\ S_2' &= -\zeta\omega_n-\omega_n(\zeta^2-1)^{1/2}, \end{aligned}$$

$HG^*(z)$: z-function of $H(S)G(S)$.

We can now obtain the frequency response of the system by substituting $z = \exp(j\omega\tau)$ into Eq. (30) as follows;

$$G_t^*(\varepsilon^{j\omega\tau}) = R_e + jI_m \qquad \cdots\cdots(31)$$

where

$$\begin{aligned} R_e &= l/\{M_1(p^2+r^2)(q^2+r^2)\}: \text{ real part of } G_t^*(\varepsilon^{j\omega\tau}), \\ I_m &= m/\{M_1(p^2+r^2)(q^2+r^2)\}: \text{ imaginary part of } G_t^*(\varepsilon^{j\omega\tau}), \\ l &= (N_1\cos\omega\tau+N_2)(pq-r^2)+N_1 r^2(p+q), \end{aligned}$$

$$m = N_1 r(pq - r^2) - r(N_1 \cos \omega\tau + N_2)(p+q)\,,$$

$p = \cos \omega\tau - z_1\,,\quad q = \cos \omega\tau - z_2\,,\quad r = \sin \omega\tau\,,$

$\omega = 2\pi f\,,\quad j = (-1)^{1/2}\,,$

f: frequency of v_r.

5. Numerical Calculations and Experimental Results

In order to investigate the appropriateness of the above theoretical method, we compare its numerically calculated results with the experimental results. The experiment is carried out on a small size dc motor. The specification of the motor and the circuit parameters are shown in Tables 1 and 2, respectively.

Table 1. Specification of dc motor

Type (Maker)	JKMM-6EM (Yasukawa Electric Co.)
Rated power	190 [W]
Rated voltage	40 [V]
Rated current	6 [A]
Rated speed	3000 [rpm]
Field excitation	Parmanent magnet

Table 2. Circuit parameters

Mechanical parameters		Electrical parameters	
Kt=0.096	[N.m/A]	E=40	[V]
Kv=0.096	[V.s/rad]	Eb=1.02	[V]
F=0.000451	[N.m.s/rad]	Edf=0.757	[V]
J=0.000282	[Kg.m]	Eth=0.792	[V]
Q=0.0806	[N.m]	C=30.6	[mF]
Qs=0.0911	[N.m]	G=0.0489	[S]
		Iq=0.840	[A]
		L=1.4, 42.6, 108	[mH]
		R=5.96	[Ω]
		τ=1/60	[s]

5.1 Steady cahracteristics.

In Figs. 4 and 5, the instantaneous waveforms of i and v in the steady state are presented for L=42.6 and 108 mH, respectively, where α=0.4. In Fig. 4, the current i flows interruptedly, but in Fig. 5 it flows continuously and is fairly

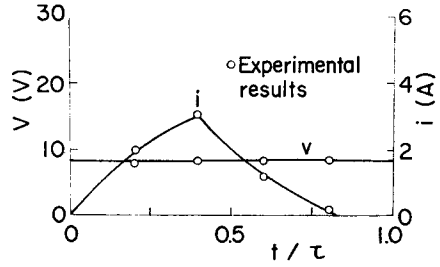

Fig. 4. Steady state waveforms of i and v for α=0.4 and L=42. 76 mH.

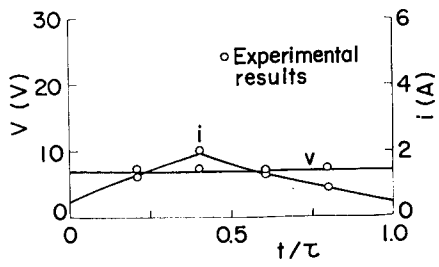

Fig. 5. Steady state waveforms of i and v for α=0.4 and L=108 mH.

smoothed by the aid of the large inductance L. From the figures, it is seen that the fluctuation of v is very small and the relations of $v \fallingdotseq V_d$ are satisfied. This is caused by the large value of J, i.e. C.

The calculated relations of V_d, I_d, I_{rms}, P_i, P_0 and η_e vs. α for L=1.4, 42.6 and 108 mH are shown in Figs. 6, 7 and 8, respectively. From these figures, we know that the motor can't keep rotating, and so $V_d=0$ when $\alpha<0.13$ and $I_d<I_q$.

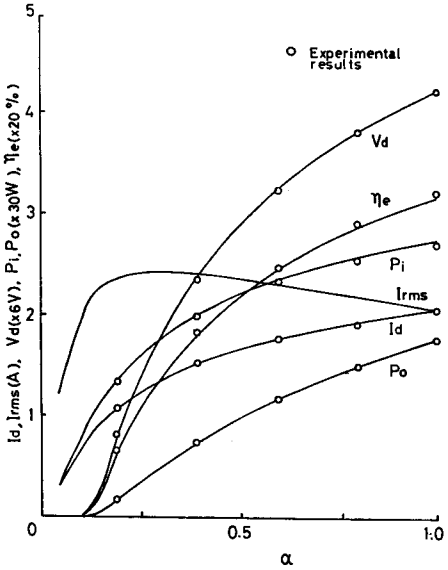

Fig. 6. Relations of V_d, I_d, I_{rms}, P_i, P_o and η_e v.s. α for L=1.4 mH.

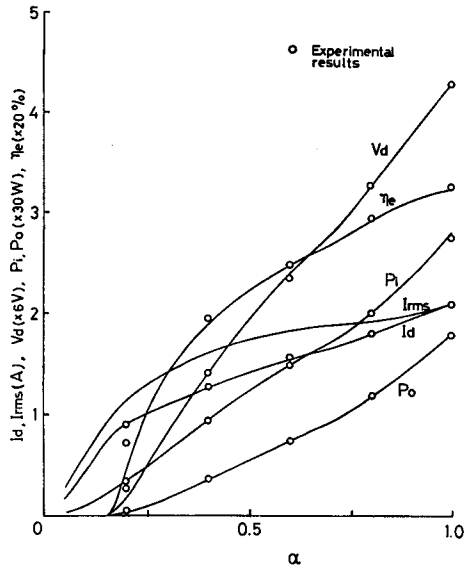

Fig. 7. Relations of V_d, I_d, I_{rms} P_i, P_o and η_e v.s. α for L=42.6 mH.

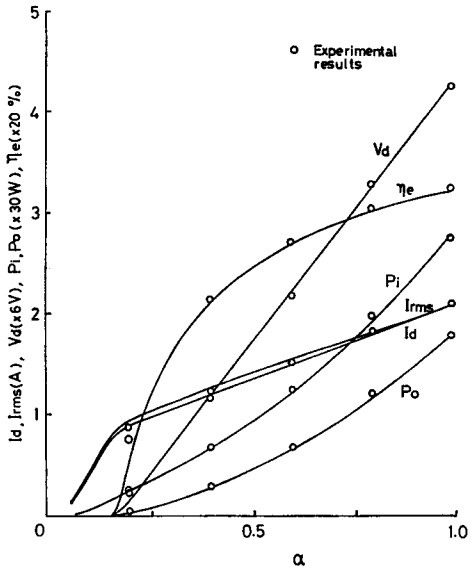

Fig. 8. Relations of V_d, I_d, I_{rms}, P_i, P_o and η_e v.s. α for L=108 mH.

Also, i flows interruptedly when $0.13 \leq \alpha < 1$ in Fig. 6 and $0.13 \leq \alpha < 0.75$ in Fig. 7. When the value of L is small and i flows intermittently, the ohmic loss $R \times I_{rms}^2$ increases, and so the efficiency η_e lowers. On the other hand, when the value of L is large and i is sufficiently smoothed, a good efficiency is obtained, as shown in Fig. 8.

In Figs. 4 to 8, some experimental results are marked, which agree well with the calculated results.

5.2 Transient characteristics.

In Fig. 9, (a) and (b), we show the calculated and experimental transient waveforms of e, i and v for $L=108$ mH, $\alpha=0.56$, and $V_d \fallingdotseq 12$ V. Next, in Fig. 10,

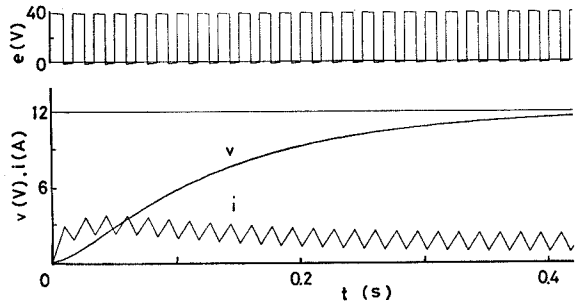

Fig. 9(a). Calculated waveforms.

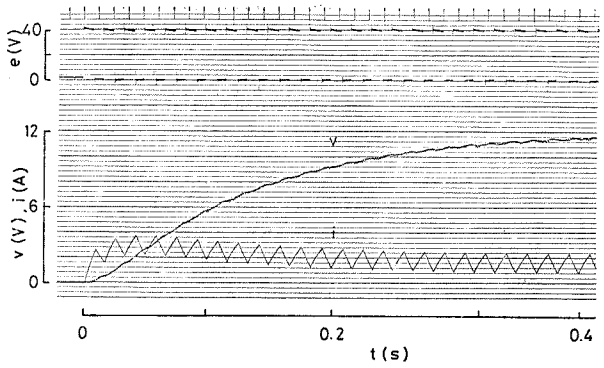

Fig. 9(b). Experimental waveforms.

Fig. 9. Transient waveforms of e, i and v for $\alpha=0.56$ and $L=108$ mH.

(a) and (b), there are plotted the waveforms for $v_r=12$ V, $K_c=0.18$ and $K_b=1$, where the motor is driven with the feedback control system, as shown in Fig. 3. The waveforms in Fig. 10(a) are calculated by substituting the relation $\alpha=K_c(v_r-v^{+0})+0.13$ into Eqs. (14), (15) and (16). In these figures, we limit the range of α as $0.13 \leq \alpha < 0.95$, so that the chopper operation is performed.

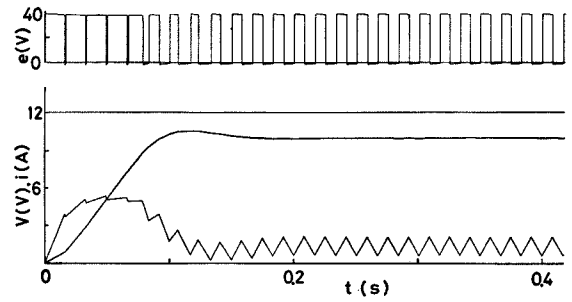

Fig. 10(a). Calculated waveforms.

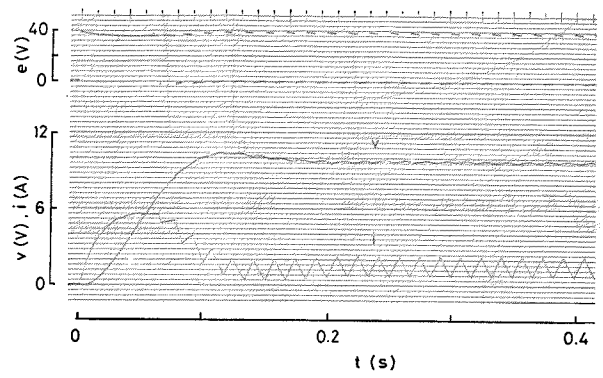

Fig. 10(b). Experimental waveforms.

Fig. 10. Transient waveforms of e, i and v for $v_r=12$ V, $\alpha=0.18\times(v_r-v^{+0})+0.13$ and $L=108$ mH.

Comparing the transient characteristics in Fig. 9 with those in Fig. 10, we can see that the motor responds quickly in the case where the motor is driven with the feedback control system. However, some offset $\varepsilon=v_r-v$ remains in the steady state, which may be decreased by increasing the value of K_c.

As seen in Figs. 9 and 10, a good agreement between the calculated results and the experimental ones is obtained.

5.3 Transfer function and frequency response.

The relations of K_m, ζ and ω_n v.s. α for $L=1.4$, 42.6 and 108 mH, which concern the transfer function $G(S)$ in Eq. (28), are given in Figs. 11, 12 and 13, respectively. As seen in Fig. 13, K_m, ζ and ω_n are independent on α, where i flows continuously. On the other hand, Figs. 11 and 12 show that those values fairly change with α, where i flows intermittently. Furthermore, $C'=C/\beta$ and $L'=L/\beta$ increase, and so the response of the motor to a change of v_r is fairly delayed.

The calculated frequency responses of the motor for $L=1.4$, 42.6 and 108 mH

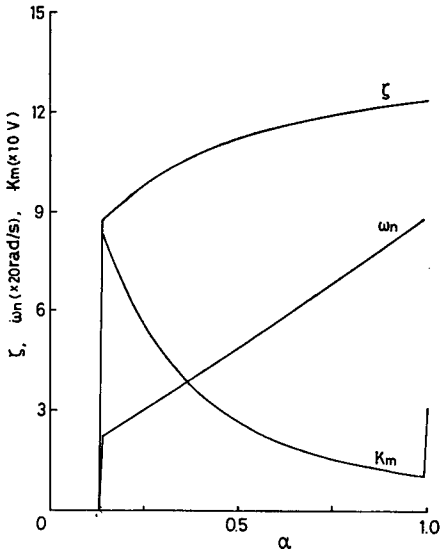

Fig. 11. Relations of K_m, ζ and ω_n v.s. α for $L=1.4$ *mH*.

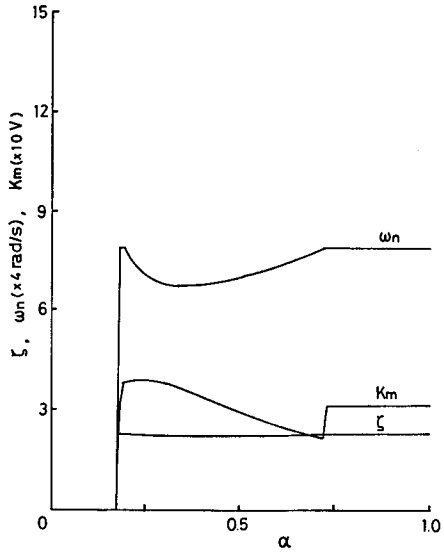

Fig. 12. Relations of K_m, ζ and ω_n v.s. α for $L=42.6$ *mH*.

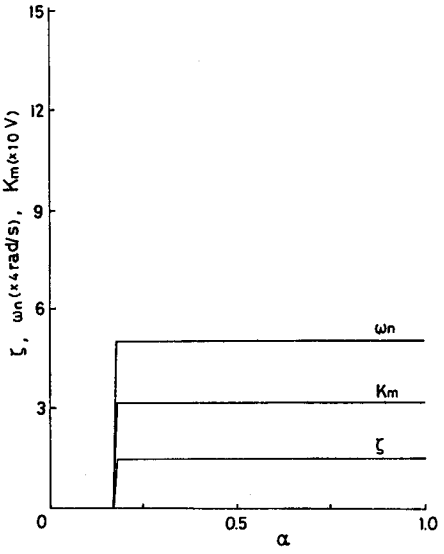

Fig. 13. Relations of K_m, ζ and ω_n v.s. α for $L=108$ *mH*.

are shown in Figs. 14(a), 15(a) and 16(a), respectively, where $K_c=0.18$, $K_b=0$ and the average values of v_r are regulated to prepare $V_d \fallingdotseq 12$ *V*. In these figures, some experimental results are shown, which agree well with the calculated results.

Next, the calculated frequency response for $L=1.4$, 42.6 and 108 mH are shown in Figs. 14(b), 15(b) and 16(b), where the motor is driven with the feedback

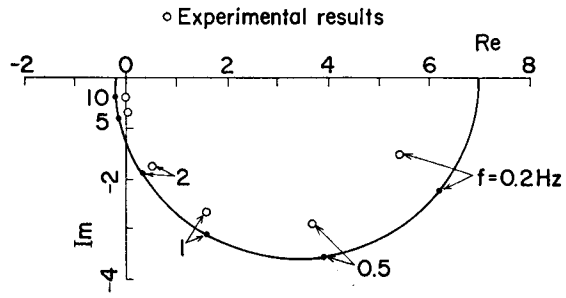

Fig. 14(a). $K_b=0$, $K_c=0.18$, $K_m=31.1$, $\zeta=1.44$, $\omega_n=19.8$.

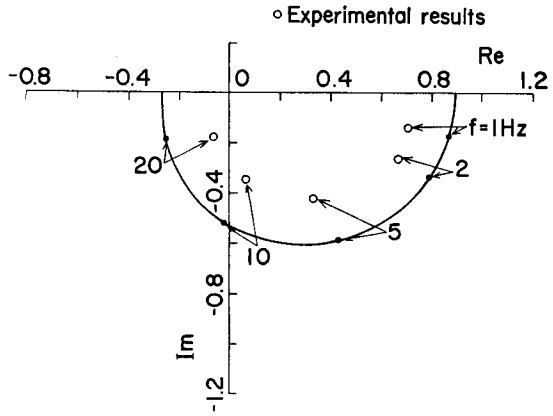

Fig. 14(b). $K_b=1$, $K_c=0.18$, $K_m=45.9$, $\zeta=10.2$, $\omega_n=68.1$.

Fig. 14. Frequency response for $L=1.4$ *mH*.

control system, and $K_b=1$ and $v_r=12+\sin(2\pi ft)$. In these figures, the experimental results deviate a little from the calculated results. This is mainly caused by the existence of the ripple component of v, which can be observed from the waveforms of v shown in Figs. 9(b) and 10(b).

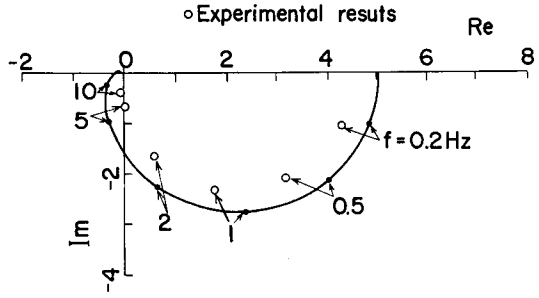

Fig. 15(a). $K_b=0$, $K_c=0.18$, $K_m=27.2$, $\zeta=2.23$, $\omega_n=28.6$.

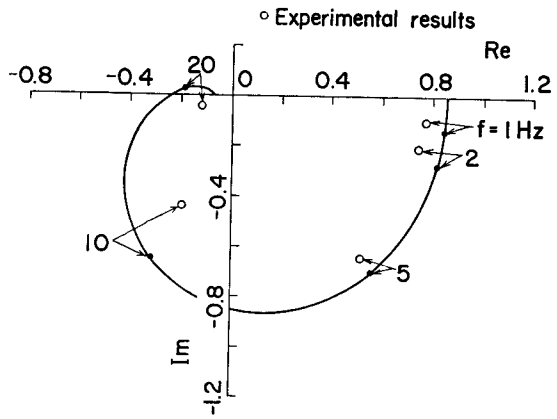

Fig. 15(b). $K_b=1$, $K_c=0.18$, $K_m=29.8$, $\zeta=2.22$, $\omega_n=27.8$.

Fig. 15. Frequency response for $L=42.6$ mH.

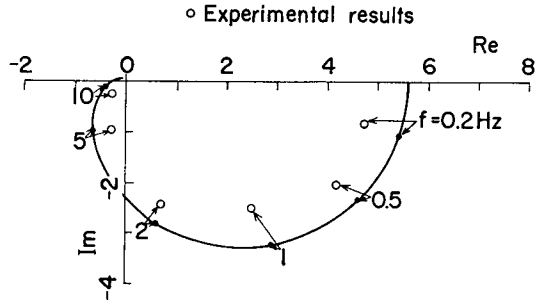

Fig. 16(a). $K_b=0$, $K_c=0.18$, $K_m=31.1$, $\zeta=1.44$, $\omega_n=19.88$.

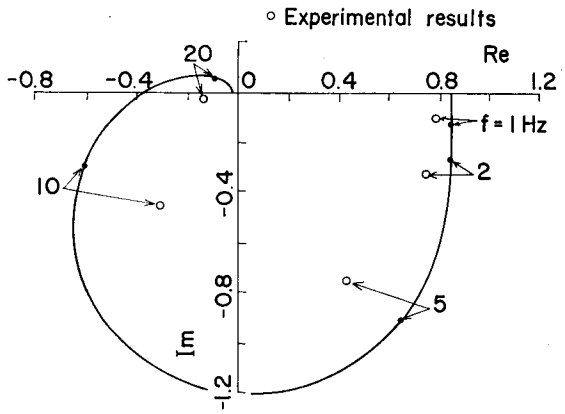

Fig. 16(b). $K_b=1$, $K_c=0.18$, $K_m=31.1$, $\zeta=1.44$, $\omega_n=19.8$.

Fig. 16. Frequency response for $L=108$ *mH*.

6. Conclusions

A theoretical method to analyse the steady and dynamic characteristics of a separately excited dc motor controlled by a thyristor chopper circuit was introduced. Also, the characteristic equation in the control circuit was derived theoretically. It was then denoted that the circuit performance was described by an equivalent sampled data system including a zero order holding circuit.

Next, the steady and dynamic characteristics were examined with a small sized actual dc motor. Then, the validity of the theoretical method was verified by ascertaining that the calculated results agree sufficiently well with the experimental results. Also, the influence of the circuit parameters and the situation of an armature current flow on the moter performances were investigated.

Furthermore, the sampled data system was applied to investigate the frequency response of the motor in the case where the motor speed is controlled with or without feedback.

Acknowledgements

The authors wish to thank Messrs. N. Amada of the Keihan Electric Railway Co. and H. Sugihara of the Chugoku Electric Power Co. for their help in the experiment and with the numerical calculations.

Refeences

1) R. Parimelalagan and V. Rajagopalan; IEEE Trans. on IGA, **IGA 7**, No. 1, 101 (1971).
2) T. Ando and J. Umoto; THIS MEMOIRS, **34**, 103 (1972).
3) T. Ando and J. Umoto; THIS MEMOIRS, **37**, 141 (1975).
4) A. Mogi; 'Synchros and Servomotors', Nikkan Kogyo Newspaper Office, Tokyo, 111 (1966).
5) B. Kondo; 'Principles of Control Engineering', Coronasha, Co., Tokyo, 127 (1977).